

# Morphology and Thermal Behavior of Dicyanate Ester-Polyetherimide Semi-IPNS Cured at Different Conditions

I. HARISMENDY,<sup>1</sup> M. DEL RÍO,<sup>1</sup> A. ECEIZA,<sup>1</sup> J. GAVALDA,<sup>2</sup> C. M. GÓMEZ,<sup>3</sup> I. MONDRAGON<sup>1</sup>

<sup>1</sup> Dpto. Ing. Química y M. Ambiente. Escuela Ingeniería T. Industrial. UPV/EHU. Avd. Felipe IV, 1 B. 20011 San Sebastián/Donostia, Spain

<sup>2</sup> Departament de Química Física e Inorgànica. Universitat Rovira y Virgili, Plaça Imperial Tàrraco, 1, 43005 Tarragona, Spain.

<sup>3</sup> Departament de Química Física. Universitat de Valencia, E-46100 Burjassot, Valencia, Spain

Received 26 April 1999; accepted 14 September 1999

**ABSTRACT:** A high-temperature thermosetting bisphenol-A dicyanate, BADCy was modified with polyetherimide, PEI, at various compositions. Phase separation and rheokinetics through curing were studied by optical microscopy, dynamic and isothermal differential scanning calorimetry, and rheological measurements. The PEI phase separated at the early stages of curing, well before gelation, and did not affect the polycyclotrimerization kinetics. The phase structure and thermal properties of the final network were investigated as a function of the PEI content and cure temperature. For this purpose, dynamic mechanical analysis, scanning electron microscopy studies, and thermogravimetric analysis were carried out. The morphological changes were interpreted in terms of a spinodal decomposition mechanism in the composition range studied. © 2000 John Wiley & Sons, Inc. *J Appl Polym Sci* 76: 1037–1047, 2000

**Key words:** cyanate esters; polyetherimide; phase separation; morphology; thermal properties

## INTRODUCTION

Cyanate ester matrices have attracted increasing attention in the electronic and composite industries because of such excellent properties as low dielectric losses, good adhesive properties, glass transition temperatures in the range of 250–300°C, processability, solubility in ketone solvents, and low moisture absorption.<sup>1–3</sup> Although cyanates are known to be relatively tough compared with other thermosetting matrices,<sup>3</sup> some applications require improved fracture resistance.

Phase separated blends of thermosets, TS, and thermoplastics, TP, have shown a higher improvement of fracture toughness with respect to that for the neat thermosetting matrix than that appearing in miscible TS/TP blends.<sup>4</sup> The properties of these types of mixtures are closely related to their generated morphology, which is controlled by the content of thermoplastic and the curing conditions. Indeed, when reaction-induced phase separation produces thermoplastic-rich particles dispersed in the continuous matrix, the toughness improvement is usually poor, but, when co-continuous or phase-inverted microstructures are formed, the fracture toughness can be dramatically improved.<sup>5–8</sup>

In this study, semi-interpenetrating polymer networks (semi-IPNs) have been synthesized

---

Correspondence to: I Mondragon.

*Journal of Applied Polymer Science*, Vol. 76, 1037–1047 (2000)  
© 2000 John Wiley & Sons, Inc.

based on a high-temperature thermosetting dicyanate ester and a thermoplastic, polyetherimide. In these initially homogeneous mixtures, as cure proceeds, the decrease of the configurational entropy attributable to the increase in molecular weight of the cyanate matrix is the main impetus for phase separation. The fracture toughness of these matrices can be improved by rubber incorporation, but at the expense of high temperature performance.<sup>9</sup> The use of a high-performance thermoplastic such as PEI has the additional advantage, as compared to rubber modification, that there is no reduction in thermal and mechanical properties of the cyanate matrix.

The aim of this work was to study the effects of cure temperature and PEI content on the chemorheology of curing as well as on the morphology and on the related final properties of a dicyanate ester semi-IPN cured by using a blend of nonylphenol and copper (II) acetylacetonate as catalysts.

## MATERIALS AND METHODS

### Materials

The dicyanate ester used in this study was a bisphenol-A dicyanate (BADCy) with the trade name AroCy B10, 99.5% purity, and with a cyanate equivalent of 139 g/eq. The selected thermoplastic was a commercial grade polyetherimide, PEI (Ultem 1000) from General Electric ( $M_n = 12000$ ;  $M_w = 30000$ ).<sup>10</sup> The catalyst system used was a mixture of 1.78 wt% of copper (II) acetylacetonate,  $\text{Cu}(\text{AcAc})_2$ , in nonylphenol, NP, both from Aldrich. We have previously reported that this amount of catalyst gives a high reaction rate, which minimizes losses of the monomer during curing.<sup>11</sup>

### Mixing and Curing Procedure

Modified cyanate resins containing 0–20 wt% PEI were prepared as follows. PEI was dissolved in methylene chloride ( $\text{CH}_2\text{Cl}_2$ ) and mixed with the resin at room temperature. The solution was heated in an oil bath at 80°C to drive off most of the solvent, and the residual solvent was removed under vacuum at 110°C for 2 h. The mixtures were cooled to 90°C, blended with the catalytic system consisting of  $\text{Cu}(\text{AcAc})_2$  at a concentration of 360 ppm and NP at a concentration of 2 wt% of

the resin weight, and stirred for 5 min to obtain a homogeneous mixture.

The mixtures were precured for 3 h at three different temperatures, 140, 160, and 180°C, and then postcured for 2 h at 200°C and 1 h at 250°C.

### Differential Scanning Calorimetry

Differential Scanning Calorimetry (DSC) measurements were performed with a Perkin-Elmer DSC-7. The DSC was calibrated with high-purity indium. Eight to ten milligrams of samples were weighed into small DSC aluminum pans, sealed with holed aluminum lids, and experiments were conducted under a nitrogen flow of 20 cc  $\text{min}^{-1}$ .

### Rheological Measurements

A Metravig Viscoanalyzer with an annular pumping device was employed for rheological measurements. Around 4 g of the catalyzed sample were introduced in a steel cylinder of 10-mm diameter. Oscillatory flow measurements were made with a device of 1-mm diameter. The storage ( $G'$ ) and loss modulus ( $G''$ ), or the loss factor ( $\tan \delta$ ) were monitored at frequencies of 5, 10, 20, and 50 Hz during the isothermal cure reaction.

### Optical Microscopy

Cloud points were determined by transmission optical microscopy (TOM), using an Olympus BHT-M model, with a Mettler heating and cooling device, Model FP82. Cloud point temperatures,  $T_{cp}$ , of the initial mixtures were determined by heating the sample until a homogeneous mixture was obtained, holding for 2 min, and then decreasing the temperature at a rate of 1°C  $\text{min}^{-1}$ .  $T_{cp}$  was taken at the onset time of the transmitted light intensity change. Isothermal experiments were carried out from 130 to 180°C at 10°C intervals to determine the cloud point time,  $t_{cp}$ . The final time of the light-transmission decrease was taken as the time to the end of phase separation,  $t_{cpF}$ . The samples were quenched, and the cloud point conversions were determined by DSC.

### Dynamic Mechanical Analysis

Dynamic mechanical analyses (DMAs) were carried out at 10 Hz and a heating rate of 3°C  $\text{min}^{-1}$  using a Metravig Viscoanalyzer. Measurements were performed using a three-point bending device with a 44-mm span. The specimen dimensions were 60 × 12 × 5 mm. The storage ( $E'$ ) and

loss modulus ( $E''$ ), or loss factor ( $\tan \delta$ ), were measured from 20°C to a temperature beyond that for the attainment of the rubbery state was attained. The glass transition temperature,  $T_g$ , was defined as the temperature corresponding to the maximum value of the loss factor.

### Scanning Electron Microscopy

The morphology of the semi-IPNs was investigated by scanning electron microscopy (SEM) Jeol JSM 35 CF. After being polished, samples of 5 and 10 wt% PEI contents were etched with  $\text{CH}_2\text{Cl}_2$ , and those of 15 and 20 wt% PEI with  $\text{H}_2\text{SO}_4$ , and then coated with a fine gold layer.

### Thermogravimetry

A Setaram 92-12 Thermobalance was used for thermogravimetric analysis (TGA). Cured samples, approximately 3 mg in weight, were scanned from 30 to 1000°C at a heating rate of 10°C.min<sup>-1</sup> under an argon flow of 20 cc min<sup>-1</sup>.

## RESULTS AND DISCUSSION

To understand how the morphologies are obtained, before analyzing the microstructures of the modified BADCy/PEI mixtures, both phase separation and kinetics of curing of mixtures with several PEI contents were investigated.

### Rheokinetics of Curing

Dynamic heating experiments were carried out from 35–400°C at a heating rate of 10°C.min<sup>-1</sup>. Figure 1 shows the exotherm peaks corresponding to the polycyclotrimerization of BADCy with PEI contents from 0 to 20 wt%. The temperature of the polymerization peak,  $T_{\text{max}}$ , was in the same temperature range for all the mixtures. The heat of reaction was independent of the PEI content,  $95 \pm 5$  kJ/cyanate equiv., in agreement with the literature data for neat cyanate resins.<sup>3</sup> This means that the presence of the thermoplastic did not affect the maximum conversion attained in the polymerization or the cure kinetics in the dynamic conditions used.

Isothermal curing was carried out from 130 to 180°C at intervals of 10°C. All samples were then subjected to a dynamic DSC scan to determine the residual heat of reaction,  $\Delta H_{\text{res}}$ .

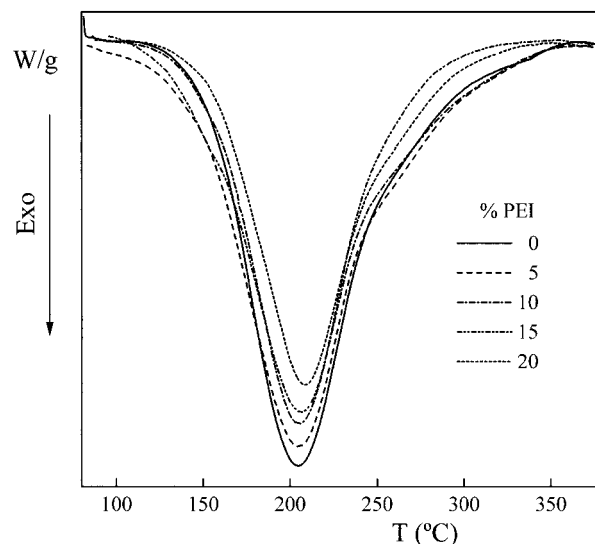


**Figure 1** Dynamic DSC scans for the BADCy/PEI mixtures with 0–20wt% PEI content.

The conversion of each sample under isothermal conditions was calculated by:

$$X = (\Delta H_{\text{iso}})_t / (\Delta H_{\text{iso}} + \Delta H_{\text{res}}) \quad (1)$$

where  $(\Delta H_{\text{iso}})_t$  is the heat of reaction at a time  $t$  calculated from the isothermal mode, and  $(\Delta H_{\text{iso}} + \Delta H_{\text{res}})$  is the total heat of reaction obtained by adding the total heat from the isothermal mode,  $\Delta H_{\text{iso}}$ , and the residual one,  $\Delta H_{\text{res}}$ . This value was  $100 \pm 5$  kJ/cyanate equiv., independent of the PEI content, and was in the same range to that obtained in the dynamic experiments.

Figure 2a reports the conversion profiles during curing at 150°C for the resin modified with several amounts of PEI. Despite the dilution effect usually seen for thermoplastic modification of thermosetting resins, no variations in cure kinetics were observed. As shown in Figure 2b, no either significant variations were presented by the 20 wt% PEI-modified matrix cured at temperatures ranging from 130–170°C, because the conversion values were similar to those corresponding to the neat resin. As we have previously shown for the catalyzed resin,<sup>12</sup> curing proceeds by means of a second-order kinetics with diffusion effects evident well before vitrification.

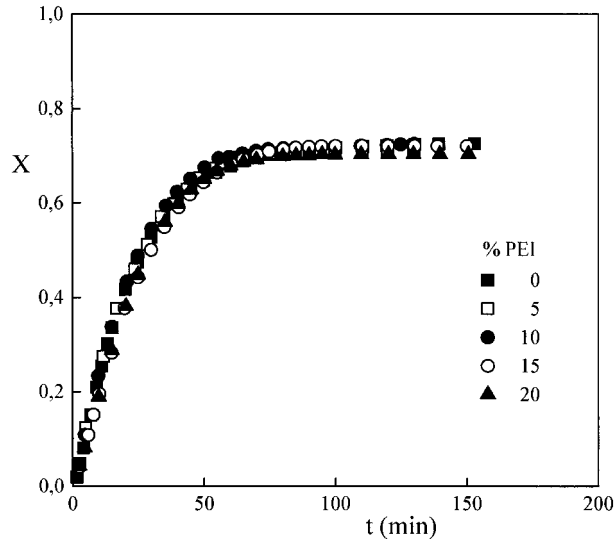
Rheological measurements were also performed at the same temperature range for samples with 0–20 wt% PEI content. The gelation time was calculated as the time where the loss factor,  $\tan \delta$ , was independent of frequency using

multiwave time tests.<sup>13</sup> The presence of PEI did not affect the gelation time of the resin. Samples were quenched at the gelation times to determine the gelation conversions by DSC.

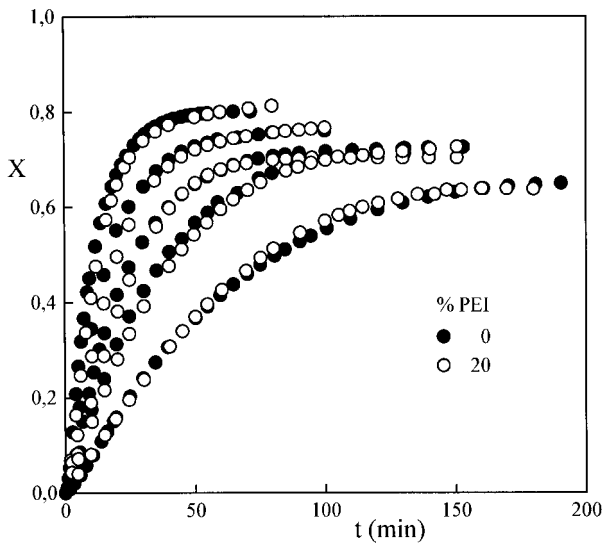
The conversion of the partially reacted samples was calculated by:

$$X = 1 - (\Delta H / \Delta H_0) \quad (2)$$

where  $\Delta H$  is the heat of reaction of the partially reacted sample, and  $\Delta H_0$  is the heat of reaction of



(a)



(b)

**Figure 2** (a) Conversion versus curing time for the BADCy/PEI mixtures with 0–20 wt% PEI content cured at 150°C; and (b) conversion versus curing time for neat BADCy and a modified mixture with 20 wt% PEI content at different curing temperatures.

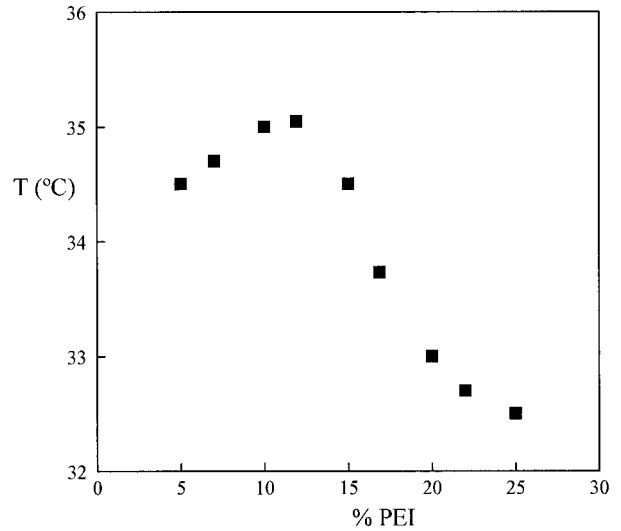
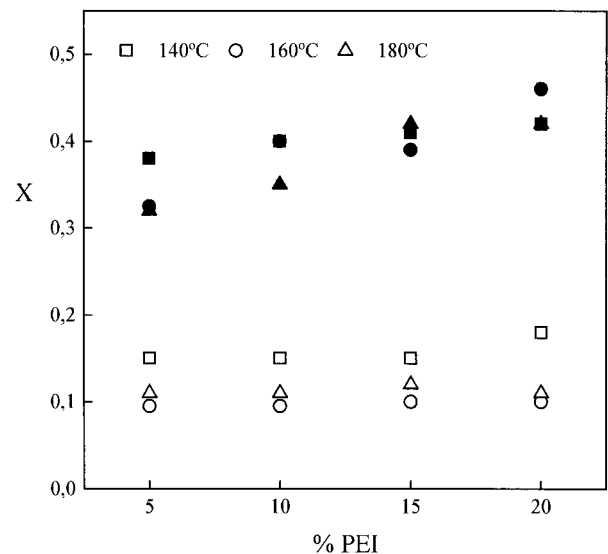


**Figure 3** Cloud point curve for the unreacted mixtures BADCy /PEI.

the initial formulation. The conversion at gelation times was between 0.58 and 0.61 for all the mixtures, similar to that found in the literature survey.<sup>14,15</sup>

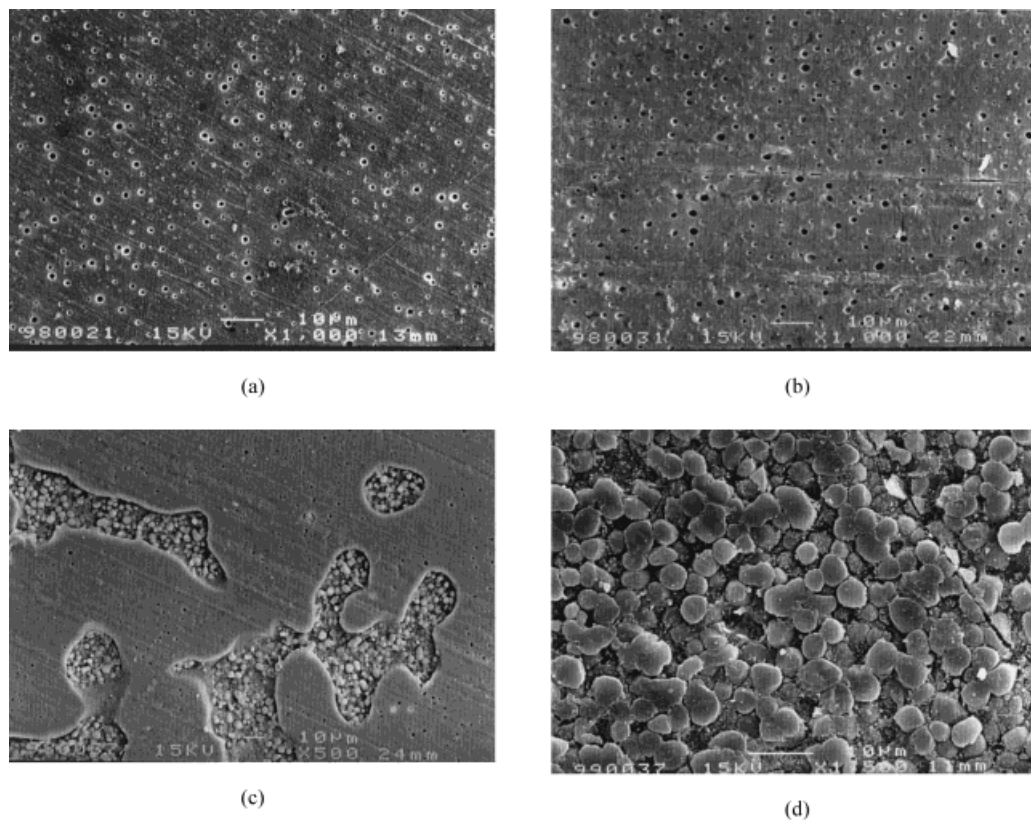
**Phase Separation Behavior**

Figure 3 shows the cloud point curve (CPC) for the unreacted mixtures as a function of PEI con-



**Figure 4** Cloud point conversions for the mixtures BADCy /PEI cured at 140°C, 160°C, and 180°C. Open points represent the cloud conversion at the onset of phase separation,  $X_{cp}$ , and filled points represent that for the end of phase separation,  $X_{cpF}$ .





**Figure 5** Morphologies of the BADCy/PEI mixtures precured at 160°C with (a) 5 wt%, (b) 10 wt%, (c) 15 wt%, and (d) 20 wt% of PEI.

tent. The BADCy/PEI mixtures exhibited an upper-critical-solution temperature (UCST) behavior as found by Lee et al.<sup>16</sup> in the case of uncatalyzed systems, with a maximum around 12 wt% PEI content, which corresponds well with the theoretical critical concentration.<sup>17</sup>

As seen by TOM, Figure 4 reports the cloud point conversions for the beginning,  $X_{cp}$ , and also those for the end,  $X_{cp,F}$ , of phase separation during isothermal experiments at 140, 160, and 180°C as a function of PEI content. Phase separation began in the earlier stages of curing, at a conversion between 0.09 and 0.16, and finished between 0.31 and 0.47 conversion, well before gelation. The influence of polymerization temperature and PEI content is masked within the experimental error of the determination, 0.05.

#### Microstructural Analysis

SEM scans revealed the presence of two distinct phases for every mixture and cure condition used. Figures 5(a–d) present the morphologies of the BADCy/PEI mixtures precured at 160°C. The

mixture with 5 wt% PEI showed spherical domains of around 0.5–1.5  $\mu\text{m}$  diameter dispersed in the BADCy-rich matrix. When the PEI content was increased to 10 wt%, the size of the microspheres increased up to 2.0  $\mu\text{m}$ .

The 15 wt% PEI containing mixture showed a dual phase morphology, similar to that found by Lee et al.<sup>16</sup> for the same mixture but cured without catalyst, with two co-continuous phases: a cyanate-rich phase, and a PEI-rich phase. In the continuous cyanate phase, small dispersed PEI particles can be seen. There were also spherical particles of cyanate of around 2–3.0  $\mu\text{m}$  dispersed in the PEI continuous phase showing that phase inversion had occurred in this phase. This dual-phase morphology inside the PEI-rich phase is believed to be formed by a secondary phase separation in the already phase-separated domains formed by the earlier spinodal decomposition. That was a consequence of cyanate chains becoming increasingly polymerized. The composition of this mixture is closed to the critical point found in the CPC for the unreacted system (12 wt% PEI). In a system with a UCST behavior, the critical

point moves to higher temperatures and higher TP concentrations as the cure reaction progress,<sup>17</sup> but in this case, as the phase separation occurred at the earlier stages of curing, no significant variations in the critical point concentration are expected.

The 20 wt% PEI mixture showed complete phase inversion. The PEI phase formed the matrix, and the BADCy appeared as big interconnected spherical domains of around 5–7  $\mu\text{m}$  diameter. All the domains in these three types of morphologies seemed to be well defined, probably because of the low viscosity of the mixture during phase separation, which allowed to the microstructural features to be well developed.

Whereas nodular and dual phase morphologies are attributed to a spinodal decomposition,<sup>16–18</sup> some controversy still exists for explaining the phase-separation mechanism involved in the case of a spherical domain morphology. Many authors<sup>16,17</sup> associate these morphologies with a nucleation and growth mechanism (NG) via binodal decomposition. Other authors state that this mechanism is not expected to take place in any case, because it is a very slow process, the spherical domain structure is represented as arising from the evolution of an initial co-continuous structure via spinodal decomposition. Thus, Inoue et al.<sup>18</sup>, Cho et al.<sup>19</sup>, and Su et al.<sup>20</sup> attributed a spinodal decomposition to these kinds of morphologies in the case of tetrafunctional epoxy/PEI blends. Moreover, Wongshanapiboon<sup>21</sup> found similar morphologies to that for the 10 wt% PEI containing BADCy mixtures in the case of 10 wt% bifunctional epoxy/PEI blends and gave experimental evidence that a spinodal decomposition had occurred. Lee et al.<sup>16</sup> have proposed a nucleation and growth mechanism for the sea-island morphology formed for the 5 and 10 wt% PEI modified uncatalyzed cyanate matrix, stating that for these compositions, the PEI domain size decreased as the precure temperature was increased.

As depicted in Figures 6 (a–c) for the catalyzed mixtures analyzed in this study, the final morphologies were also affected by the precure conditions, especially for the 10 wt% PEI mixture. Nevertheless, the size of the dispersed particles for this composition increased for higher precure temperatures. The phase-separated small domains appearing for the semi-IPN with a 5 wt% PEI content slightly increased with precure temperature as well. These results lend support to the idea that phase separation could take place

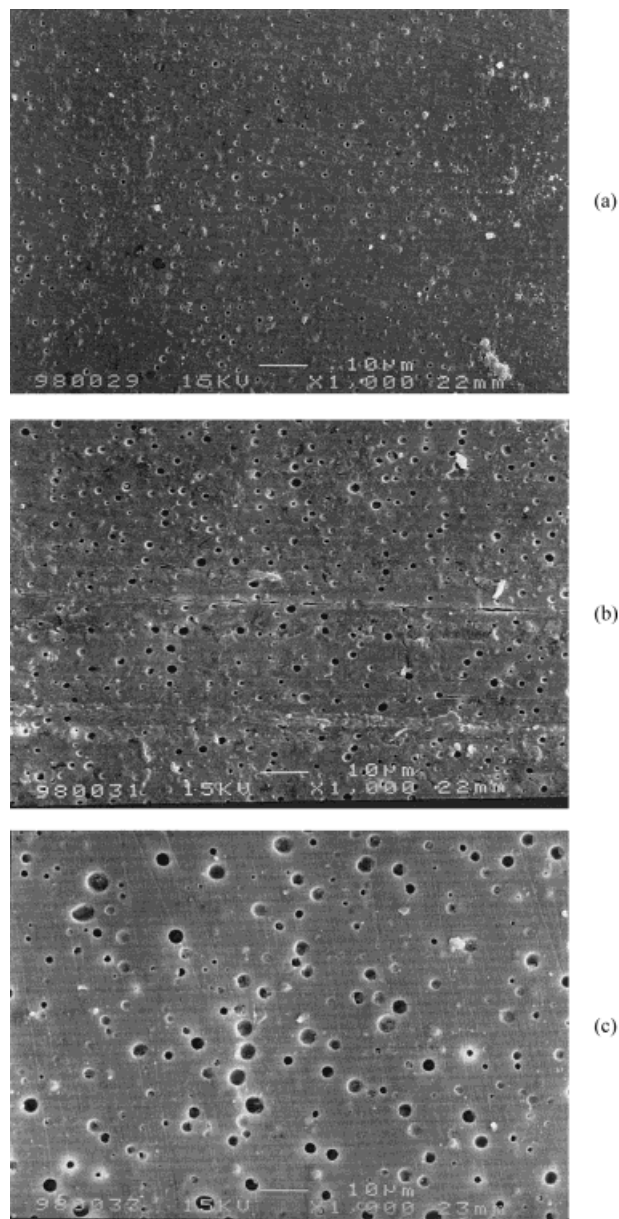


**Figure 6** Morphologies of the 10 wt% PEI containing mixtures precured at (a) 140°C, (b) 160°C, and (c) 180°C.

via the spinodal decomposition mechanism<sup>18</sup> in a way dissimilar to that shown for the uncatalyzed mixture<sup>16</sup>. Work is in progress to elucidate the exact mechanism of phase separation in these mixtures.

On the other hand, as reported in Figures 7 (a–c) for the 15 wt% PEI-containing mixture precured at 140, 160, and 180°C, respectively, the dual co-continuous microstructure seemed very similar for all the temperatures.



As shown in Figures 8 (a–c) in the case of the 20 wt% PEI mixture, there was an increase of the size of the BADCy spherical domains with the precure temperature as found by Lee et al.<sup>16</sup> for the uncatalyzed mixtures.

Finally, as shown in Figures 9 (a–c) no significant variations in the morphology were observed for the 15 wt% PEI-containing mixture at different postcure temperatures, meaning that the morphology was fixed during the early curing step.

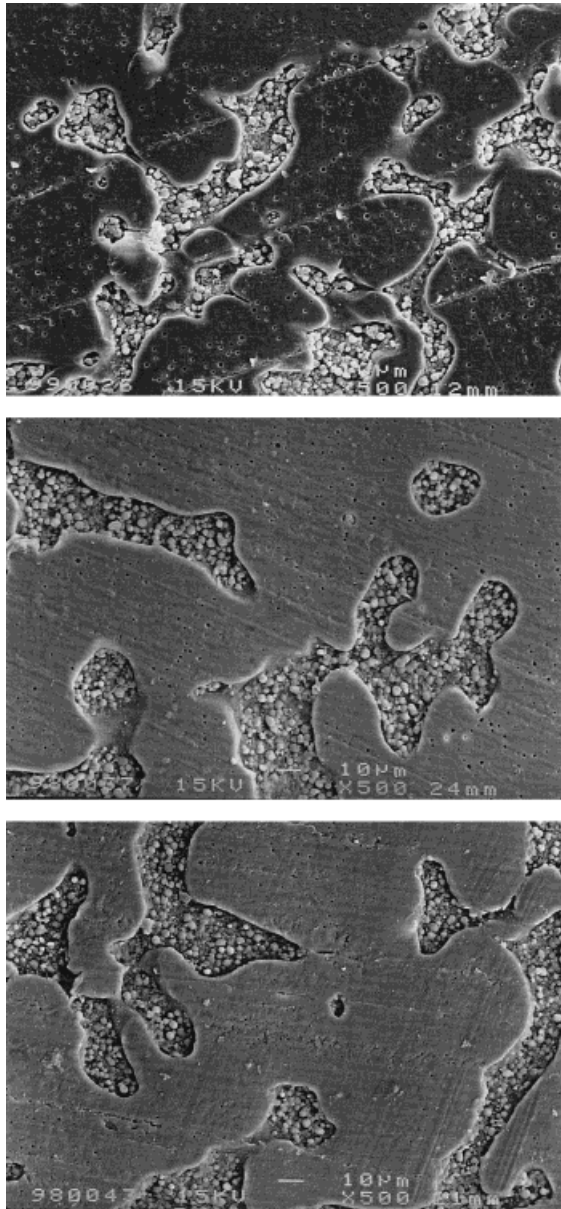


**Figure 7** Morphologies of the 15 wt% PEI containing mixtures precured at (a) 140°C, (b) 160°C, and (c) 180°C.

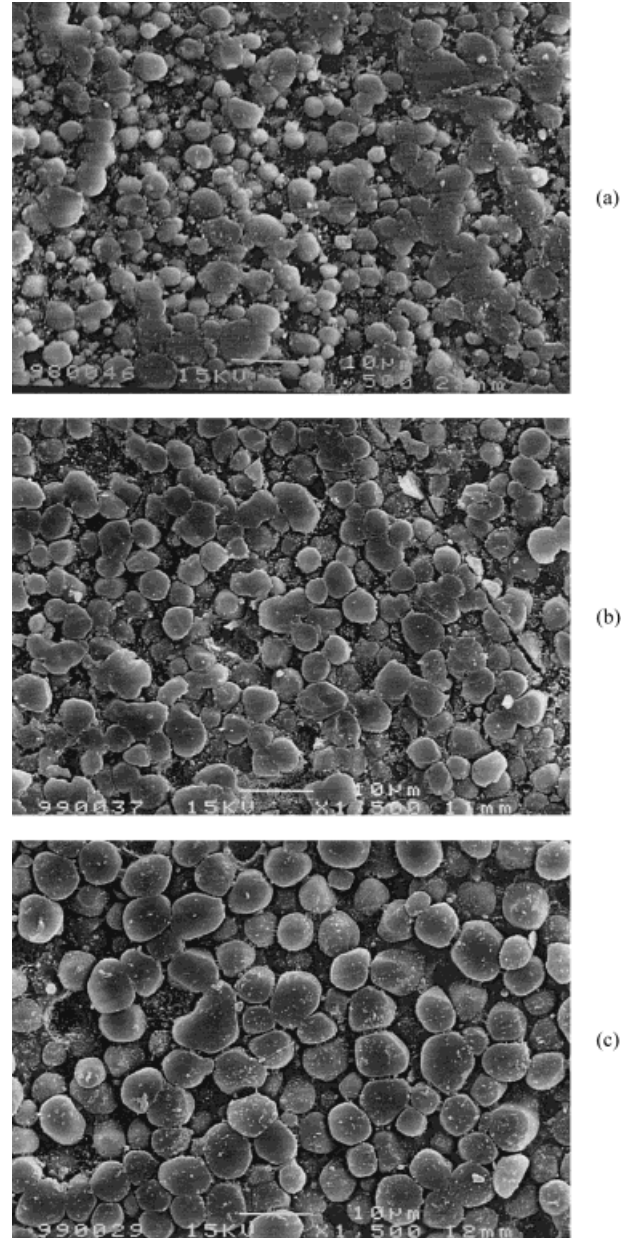


**Figure 8** Morphologies of the 20 wt% PEI containing mixtures precured at (a) 140°C, (b) 160°C, and (c) 180°C.

**Dynamic Mechanical Analysis**

Mixtures were also examined using DMA at 10 Hz, because this technique can give more information on microstructure of cured mixtures providing details about molecular mixing and phase continuity. Figure 10 (a–b) shows the storage and loss modulus variation with temperature for the BADCy/PEI blends precured at 160°C. The viscoelastic spectra exhibited two E'' relaxation

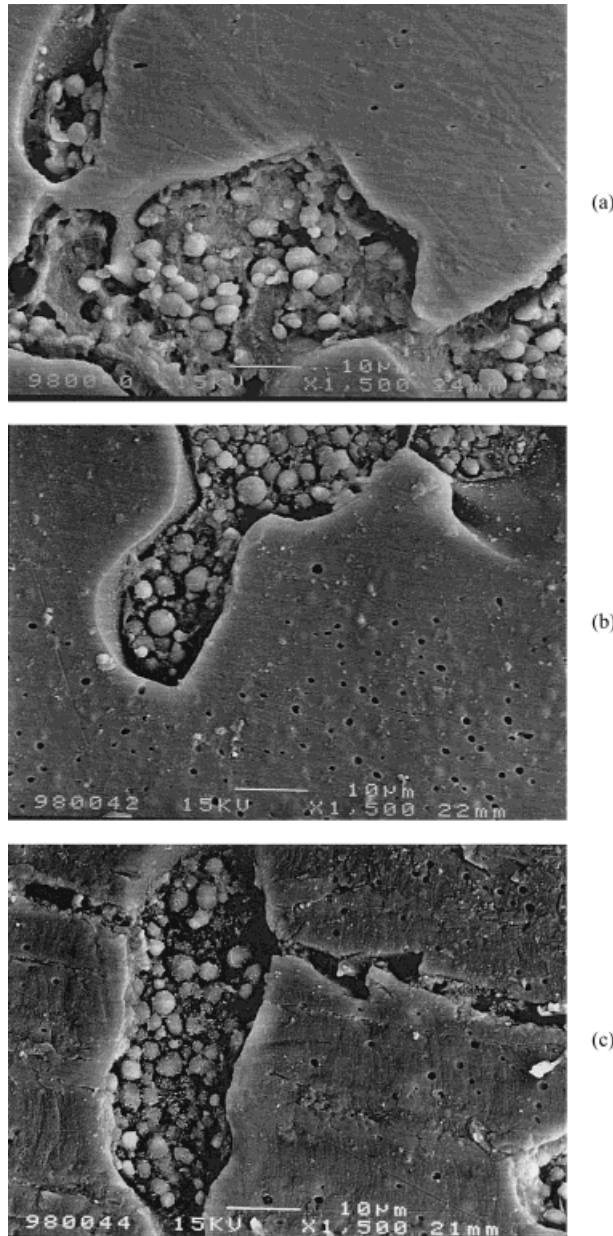
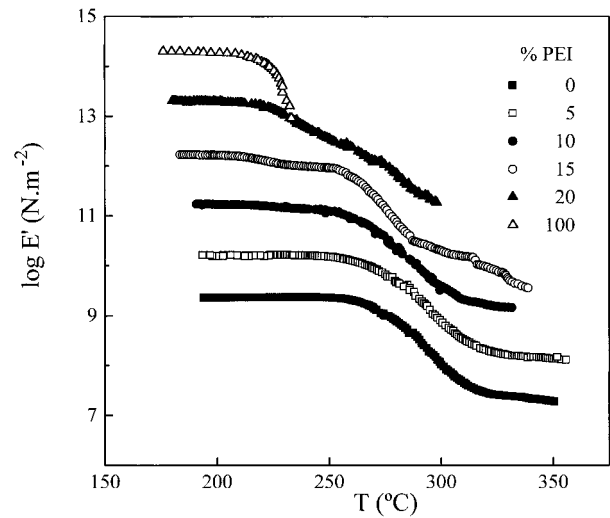


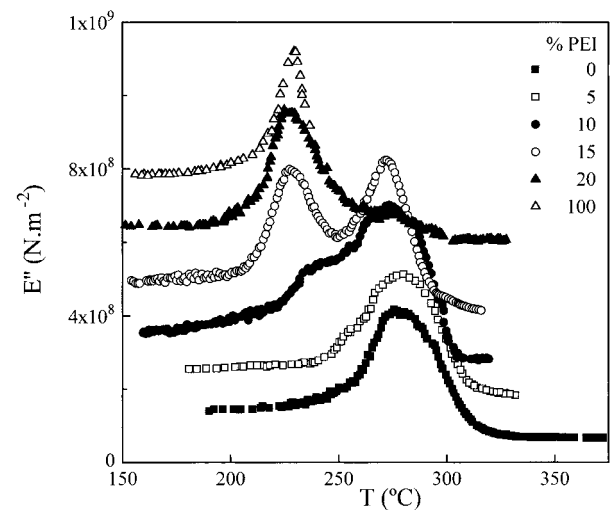
**Figure 9** Morphologies of the 15 wt% PEI containing mixtures cured at (a) 180°C, (b) 180°C/200°C, and (c) 180°C/250°C.

peaks attributable to both separated phases, which approached those of the pure components. Thus, one for the higher temperature, which corresponds to the cyanate matrix, appeared at a lower temperature than that for the uncatalyzed matrix<sup>22</sup> because of plasticization by nonylphenol<sup>23</sup>. The relative evolution of these relaxations confirmed the above shown phase inversion phenomena. As the PEI concentration was increased, the magnitude of the  $\alpha$  relaxation of the PEI-rich

phase with respect to that for the BADCy-rich phase increased. For compositions lower than 15 wt% PEI, the peak area of the BADCy-rich phase was larger than those of the PEI-rich phase, indicating that the BADCy formed the matrix in that composition range. At 15 wt% PEI content, both areas were comparable, thus confirming that



(a)



(b)

**Figure 10** (a) Storage modulus variation with temperature for the BADCy/PEI mixtures pre-cured at 160°C. The scale of  $\log E'$  is correct for the neat resin. For other compositions, the scale is offset vertically from that of its immediate neighbors by one unit; and (b) loss modulus variation with temperature for the BADCy/PEI mixtures pre-cured at 160°C. The scale of  $E''$  is correct for the neat resin. For other compositions, the scale is offset vertically from that of its immediate neighbors by  $1 \times 10^8$  unit.



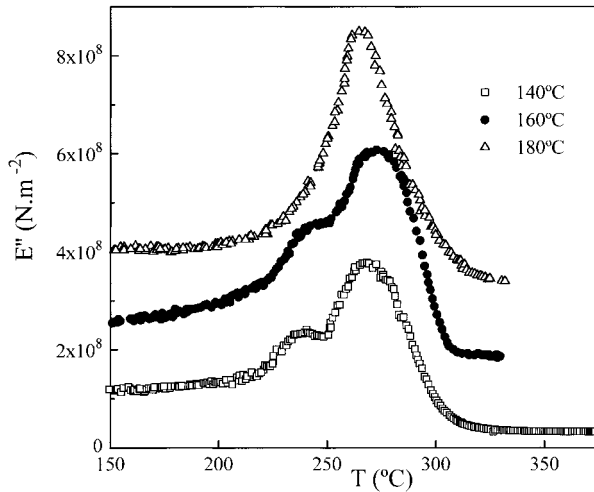


**Figure 11** Loss modulus of the 10 wt% PEI containing mixtures precured at different temperatures. The scale of  $E''$  is correct for the mixture precured at 140°C, and offset for other temperatures, as in Figure 10 (b).

this composition had a dual-phase or a nearly co-continuous morphology. At 20 wt% PEI content, the magnitude of the relaxation corresponding to the PEI-rich phase was much larger than that for the BADCy rich phase, showing that phase inversion had occurred, thus becoming the PEI-rich phase the matrix. These results are in agreement with the morphologies above reported by SEM.

Figure 11 shows the loss modulus of the 10 wt% PEI containing mixture precured at different temperatures. The shape of the relaxations changed as the precure temperature was increased, and at 180°C, a single peak was observed. Table I shows the  $T_g$ s of the BADCy-rich phase,  $T_{g_{BADCy}}$ , and the PEI-rich one,  $T_{g_{PEI}}$ , in the mixtures taken as the maximum in the loss

factor curves. Although the results were masked by the uncertainty of the technique, there seems to be a slight decrease of the  $T_g$  cyanate-rich phase with the precure temperature increase. The big size of the PEI domains at 180°C, together with the  $\alpha$  relaxations variations, could be attributed to a change in the concentration of PEI and cyanate in the phase-separated regions. This could support the fact that phase separation occurred via a spinodal decomposition. In the spinodal mechanism, the composition of the separated phases changes continuously during phase separation.<sup>18</sup> For higher precure temperatures, the kinetic constraints are higher, meaning that phase separation stops before, so that each phase has the  $T_g$  corresponding to the composition at that moment. As it can be seen in Table I, the 15 wt% PEI-containing mixtures, which showed a typical morphology of a spinodal mechanism, the relaxational behavior was similar to that observed with the 10 wt% PEI containing mixture. The  $T_g$  of the cyanate-rich phase slightly decreased as the precure temperature,  $T_c$ , was increased. Figure 12 shows the loss modulus of the 15 wt% PEI-containing mixture precured at different temperatures. As for the 10 wt% PEI-containing mixture, the relaxations moved slightly closer to one another as the precure temperature was increased.

On the other hand, although not shown, the spinodal mechanism even could happen for the mixture with a 5 wt% PEI, because the temperature corresponding to the maximum of loss modulus for the sample precured at 180°C appeared at slightly lower temperatures than those for the mixtures precured at 140 and 160°C, which should be attributable to the slight increase on domain size with precure temperature.

**Table I**  $T_g$  of the Cyanate and PEI-Rich Phases at Different Precure Temperatures,  $T_c$ , and PEI Contents.

$\rightarrow T_c$ (°C)	140		160		180	
	$T_{g_{BADCy}}$ (°C)	$T_{g_{PEI}}$ (°C)	$T_{g_{BADCy}}$ (°C)	$T_{g_{PEI}}$ (°C)	$T_{g_{BADCy}}$ (°C)	$T_{g_{PEI}}$ (°C)
0	299	—	299	—	299	—
5	299	—	298	—	296	—
10	297	235	297	236	294	—
15	295	233	294	234	291	236
20	—	233	—	233	—	234
100	—	233	—	233	—	233

Despite the increase in the size of the particles observed by SEM, no significant variations were found in the viscoelastic spectra for the mixtures with 20 wt% PEI contents precured at different temperatures. The temperature corresponding to the maximum of the  $\alpha$  relaxation of the PEI-rich phase,  $T_{g_{PEI}}$ , was in the same temperature range as that for the neat PEI, meaning that phase separation was complete, and there was no cyanate dissolved in this phase.

### Thermal Stability

Figure 13 shows the thermograms of the PEI-containing mixtures precured at 160°C. Every mixture presented a similar behavior, with onset of weight loss around 400°C. There was only a slight decrease in the amount of weight loss in the first step (cyanate decomposition) when the PEI content was increased because of the lower level of cyanate existing in the sample. The addition of PEI does not seem to affect the thermal stabilities of the mixtures in the composition range studied.

### CONCLUSIONS

A high-temperature thermosetting bisphenol-A dicyanate was modified with polyetherimide at various compositions, ranging from 0–20 wt% PEI. Physicochemical characterization of curing and phase separation has allowed us to explain

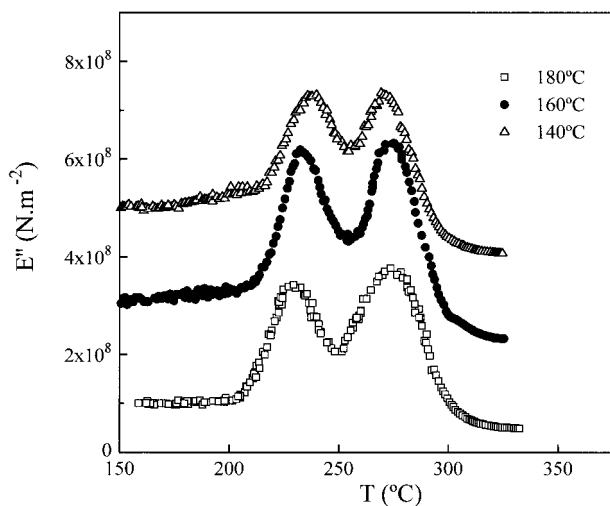


**Figure 12** Loss modulus of the 15 wt% PEI containing mixtures precured at different temperatures. The scale of  $E''$  is correct for the mixture precured at 140°C, and offset  $2 \times 10^8$  for other temperatures.

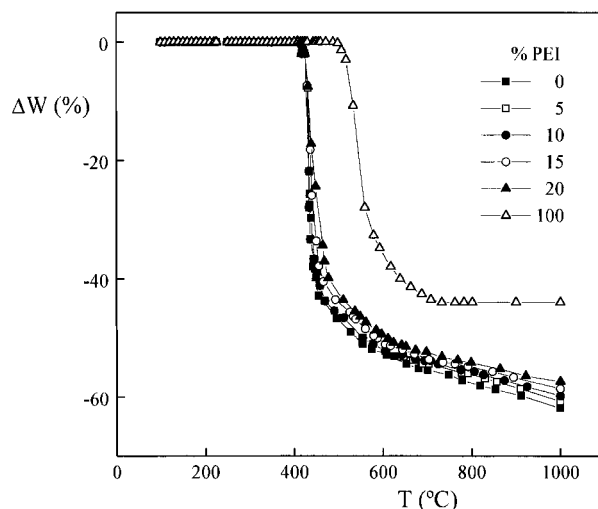


**Figure 13** TGA thermograms of the BADCy/PEI mixtures with different PEI contents precured at 160°C.

the morphological features of the PEI-modified mixtures investigated by microscopic and dynamic mechanical techniques.

The PEI phase separated at the early stages of curing, well before gelation, and did not affect the polycyclotrimerization kinetics of the BADCy resin. The uncured mixtures showed an upper critical solution temperature behavior, presenting the critical temperature at 12 wt% PEI.

When the mixtures were cured, a two-phase morphology was observed for all PEI contents. Phase inversion occurred at around 15 wt% PEI. At lower thermoplastic content, the mixtures showed PEI spherical domains dispersed in the BADCy matrix. At 15 wt% PEI, a nearly dual co-continuous morphology was observed; whereas, at 20 wt% PEI, a nodular morphology was observed, with BADCy nodules included in the PEI matrix.

The cure temperature did not influence the morphology, but the domain size and the composition of the dispersed phases did change. As cure temperature was increased, both the PEI microspheres and the BADCy nodules increased, and the PEI- and BADCy-rich phase relaxations moved closer to one another. These morphological changes seem to be attributable to a spinodal decomposition in all the composition ranges studied. Although there was a slight decrease of the  $T_g$  of the cyanate, the presence of PEI did not affect its thermal stability.

We are grateful for the financial support under Contract MAT95-0701 from Dirección General de Ciencia y

Tecnologia (DGICYT) Spain. One of the authors (I. H.) is indebted to the Ministerio de Educación y Cultura (Spain) for a fellowship grant. Thanks are also extended to Ciba Spec. Chem. Inc, for supplying the cyanate resin used in this work.

## REFERENCES

1. Shimp, D. A. *SAMPE Quart* 1987, 19, 41.
2. Mc Connell, V. P. *Adv Comp* 1992, May/June, 28.
3. Hamerton, I. In *Chemistry and Technology of Cyanate Ester Resins*; Hamerton, I., Ed.; Blackie: London, 1994; Chapter 1.
4. Chen, M. C.; Hourston, D. J.; Sun, W. B. *Eur Polym J* 1992, 28, 1471.
5. Raghava, R. S. *J Polym Sci B: Polym Phys Ed* 1987, 25, 1017.
6. Mackinnon, A. J.; Jenkins, S. D.; McGrail, P. T.; Pethrick, R. A. *Macromolecules* 1992, 25, 3492.
7. Kinloch, A. J.; Yuen, M. L.; Jenkins, S. D. *J Mater Sci* 1994, 29, 3781.
8. Venderbosch, R. W.; Meijer, H. E. H.; Lemstra, P. J. *Polymer* 1994, 35, 4349.
9. Ciao, Z.; Mechin, F.; Pascault, J. P. *Polym Int* 1994, 34, 41.
10. Bucknall, C. B.; Gilbert, A. H. *Polymer* 1989, 30, 213.
11. Harismendy, I.; Gomez, C.; Ormaetxea, M.; Martin, M. D.; Eceiza, A.; Mondragon, I. *J Polym Mater* 1997, 14, 317.
12. Harismendy, I.; Gomez, C.; Del Rio, M.; Mondragon, I. *Polym Int* in press.
13. Halley, P. J.; Mackay, M. E.; George, G. A. *High Perform Polym* 1994, 6, 405.
14. Chen, Y. T.; Macosko, C. W. *J Appl Polym Sci* 1996, 62, 567.
15. Deng, Y.; Martin, G. C. *Polymer* 1996, 37, 3675.
16. Lee, B. K.; Kim, S. C. *Polym Adv Technol* 1995, 6, 402.
17. Riccardi, C.; Borrajo, J.; Williams, R. J. J.; Girard-Reydet, R.; Sautereau, H.; Pascault, J. P. *J Polym Sci B: Polym Phys Ed*, 34 1996, 349.
18. Inoue, T. *Prog Polym Sci* 1995, 20, 119.
19. Cho, J. B.; Hwang, J. W.; Cho, K.; An, J. H.; Park, C. E. *Polymer* 1993, 34, 4833.
20. Su, C. C.; Woo, E. M. *Polymer* 1995, 36, 2883.
21. Wongshanapiboon, T. Ph.D. dissertation 1992, Cranfield Institute of Technology, Cranfield, England.
22. Porter, D. S.; Bhattacharjee, S.; Ward, T. C. *ACS Polym Div Polym Mat Sci Eng* 1998, 79, 186.
23. Zacharia, R. E.; Simon, S. L. *ACS Polym Div Polym Mat Sci Eng* 1998, 75, 209.